Generation of nonequilibrium electron and lattice temperatures in copper by picosecond laser pulses

G. L. Eesley
Physics Department, General Motors Research Laboratories, Warren, Michigan 48090-9055
(Received 11 June 1985)

Picosecond laser pulses can be used to generate and probe nonequilibrium electron and lattice temperature differences in metals. This is demonstrated by transient thermoreflectance measurements on copper in the vicinity of the *d*-band absorption edge. Our measurements are in agreement with an energy-balance model based on a separation of the one-dimensional heat-flow equation into electron and lattice subsystems.

INTRODUCTION

The generation of an electron temperature greater than the lattice temperature in a metal has been the subject of theoretical investigation for several years.[1-3] It has been postulated that if the electrons can be directly heated on a time scale shorter than the electron-phonon (*e*-ph) energy relaxation time, then a nonequilibrium temperature difference is possible because of the small specific heat of the electron gas. Although *e*-ph collision times are on the order of 10^{-14} sec at room temperature, an equilibration time of $\sim 5\times 10^{-13}$ sec would be expected for an electron with 1 eV of excess energy relaxing into lattice phonons which typically accommodate ≈ 0.02 eV.

The advent of ultrashort pulsed lasers permits the investigation of nonequilibrium heating in condensed matter. Many studies of electron-phonon relaxation have concentrated on semiconducting materials with spectral features accessible by currently available laser sources.[4] Relatively few attempts have been made to generate and observe the nonequilibrium heating of metal electrons.[3,5-7] The earliest reported evidence for this phenomenon was based on recordings of the transient blackbody radiation spectra produced by heating Cu, Ag, and Au targets with intense, 20-picosecond (psec) Nd:yttrium aluminum garnet (YAG) laser pulses.[5] Another approach to the observation of nonequilibrium heating is based on the phenomenon of multiphoton photoemission from metals illuminated by high-intensity laser pulses.[3,6-8] Optical heating of the metal produces more electrons with energies above the Fermi level, and multiphoton photoemission from the tail of the Fermi distribution can take place with the absorption of fewer photons. In the event of nonequilibrium heating, the thermally-assisted photoemission is enhanced. Yen *et al.*[3,6] demonstrated that only equilibrium heating was contributing to the photoemission signal from tungsten illuminated by 30-psec Nd:YAG laser pulses with intensities reaching 3.5 GW/cm^2. Recently, Fujimoto *et al.*[7] have found evidence for nonequilibrium heating in tungsten using 75-femtosecond (fsec) laser pulses to produce thermally-enhanced multiphoton photoemission. Their elegant pump-probe experiment demonstrated substantial thermally-assisted photoemission several hundred femtoseconds after the arrival of the heating pulse. However, an accurate determination of the electron temperature and *e*-ph coupling was hindered by the nonlinear dependence of the signal on laser intensity and problems associated with measuring peak photocurrent densities in excess of 1 kA/cm^2.

All of the previous efforts to observe nonequilibrium heating placed an emphasis on generating an extremely large electron-lattice temperature difference of ≈ 1000 K. These experiments also produce lattice temperature increases of several hundred degrees. This situation is difficult to model since the temperature dependence of the thermal conductivity, lattice specific heat, and the *e*-ph coupling must be accounted for dynamically. Because the time evolution of the electron and lattice temperature is governed by two coupled nonlinear differential equations,[1] solutions are generally obtained by numerical procedures which only account for the linear temperature dependence of the electronic specific heat. All other physical parameters are assumed to remain constant in time (temperature).[2,6-8] Thus a perturbative experiment which produces a substantially smaller electron-lattice temperature difference should be more accurately described by this method of solving the nonequilibrium heating model.

We have used picosecond laser pulses to sequentially heat a Cu sample and to probe the thermally-induced change in reflectivity in the vicinity of the *d*-band absorption edge. We have observed a rapid heating and cooling transient which follows the laser pulse and results from the heating of conduction electrons to a temperature a few degrees above that of the lattice.[9,10] Under our experimental conditions, we show that the nonequilibrium heating model predicts the generation of electron temperatures a few degrees in excess of the lattice. In addition, at different initial temperatures the qualitative features of our experimental results are in agreement with model predictions.

TRANSIENT THERMOREFLECTANCE SPECTROSCOPY

Thermoreflectance spectroscopy is an important method for studying the critical points in band structure associated with the interband optical absorption in solids. This technique belongs to a general class of modulation

 ©1986 The American Physical Society

techniques which are based on the observation that relatively small changes in a reflection (or an absorption) spectrum can be enhanced by derivative methods; that is, a measurement of the change in reflection (or absorption) due to a modulation of some physical parameter such as temperature, stress, or electric field.[11] The relatively weak onset of interband transitions can be easily observed by means of phase-sensitive detection of the modulated reflectivity. In the case of a temperature modulation, a change in reflectivity will result from thermally-induced changes in the dielectric function which can be related directly to the electronic band structure of the material. Scouler[12] was the first to demonstrate the significance of the thermoreflectance technique to band-structure studies in metals, by showing that the thermoreflectance spectrum of Au contained more detail than the conventional reflectance spectrum. Thermoreflectance spectroscopy continues to be used as a probe of band structure in condensed matter,[13] in addition to photoemission and spectroscopic ellipsometry.

The traditional approach to a thermomodulation measurement is to pass a low-frequency alternating current through an optically thin sample film, and synchronously detect the corresponding heating-induced reflectivity (or transmissivity) change as a function of optical wavelength. Temperature changes of ≈ 10 K result in observed reflectivity changes on the order of $\Delta R = 10^{-4}$.[11] A variety of effects contribute to the reflectivity change, including thermal expansion, electron-phonon collisions, and shifting of the Fermi level.[14] Scouler[12] and Rosei and Lynch[14] were the first to observe a polarity reversal of ΔR when the photon energy was tuned through the d band to Fermi-level interband transition energy of Au and Cu. This transition is a common feature of the noble-metal optical properties, and it is schematically represented in Fig. 1. Optical transitions from the top of a relatively flat

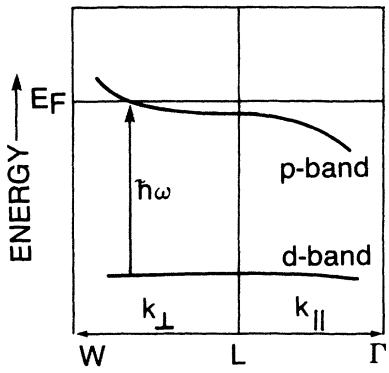

FIG 1. Schematic representation of the noble-metal band structure which is responsible for optical transitions from the top of the d band to empty conduction-band (p band) states near the Fermi level (E_F). The horizontal axis represents electron momentum and the optical transition is indicated by the vertical arrow. The transition energy is $\hbar\omega = 2.15$ eV for Cu, 2.4 eV for Au, and 4 eV for Ag.

d band to unoccupied states near the Fermi level in the conduction band (p band) are indicated by the vertical arrow. The onset of this transition occurs at a photon energy of 2.15 eV in Cu,[14] 2.4 eV in Au,[12] and 4 eV in Ag.[15] The unique polarity reversal of the thermoreflectance signal originating from this transition was interpreted as the result of Fermi distribution smearing; that is, a heating-induced increase in unoccupied states below the Fermi level and a decrease in unoccupied states above the Fermi level.[11] The details of this temperature dependence will be described in the next section. The important point to realize is that the Fermi smearing contribution to the thermoreflectance signal is a direct indication of the conduction-electron temperature.

Unfortunately, electron-phonon collisions and lattice expansion also contribute to the thermoreflectance signal in this photon-energy range. The detailed contributions can only be distinguished by measurements at temperatures sufficiently low that lattice contributions become negligible [<20 K (Ref. 16)]. Since the lattice heating proceeds by the transfer of energy from hot electrons, we may take advantage of the fact that the lattice contributions to the reflectivity change will be delayed in time relative to the purely electronic contributions (Fermi smearing). Ultrashort light pulses can be used to produce rapid heating of the metal electrons, followed by time-resolved measurements of the thermoreflectance signal. For sufficiently short pulses (≈ 1 psec), transient thermoreflectance measurements can temporally resolve electronic and lattice contributions to the reflectivity change and permit the investigation of spectral behavior as well.[9]

The laser system used for our transient thermoreflectance spectroscopy (TTRS) measurements consists of a mode-locked argon-ion laser which sychronously pumps two-ring dye lasers at a pulse repetition rate of 246 MHz. The heating dye laser is fixed in wavelength at 645 nm (1.92 eV), with an average output power of 140 mW and a pulse intensity autocorrelation of 8 psec [full width at half maximum (FWHM)] as measured by second-harmonic generation. The probing laser can be tuned between 572 and 610 nm, and after attenuation the average power at the sample is <2 mW. The probe-pulse autocorrelation is nominally 8 psec (FWHM), with an additional 1-psec broadening at the tuning extremes.

The temporal cross correlation of the heating pulse with the probing pulse is measured by two-photon absorption in GaP. This method of cross-correlation measurement yields identical results when compared with the typical second-harmonic-generation (SHG) technique.[17] The two-photon absorption method is preferable to SHG, due to ease of alignment and high signal-to-noise ratio. Phase matching of the laser beams is unnecessary, and the same detector used for the TTRS measurements can be used to detect the cross-correlation signal. Since the GaP is placed in the sample position, the zero-time-delay position of the optical delay line is also determined. The cross-correlation FWHM of the probing pulse with the heating pulse is 12 psec at a probe wavelength of 590 nm and a heating pulse wavelength of 645 nm. The relative temporal jitter between the heating and probing lasers produces a cross-correlation width in excess of the individual

pulse autocorrelations of 8 psec. Jitter times on the order of 2 psec are typical of synchronously pumped dye-laser systems.[18]

A schematic of the optical arrangement used for the TTRS measurements is shown in Fig. 2. The probe laser pulse train passes through a variable optical delay line, a polarization beam splitter, a quarter-wave plate, and is focused to a beam diameter of $\lesssim 20$ μm at the sample. The quarter-wave plate is oriented with the major axis at 45° to the probe polarization, and this produces a circularly polarized field at the sample surface. The retroreflected probe pulse is transmitted through the quarter-wave plate again. This results in a net polarization rotation of 90° relative to the incoming pulse, and thus the retroreflected probe pulse exits through the detector port of the polarization beam splitter. The detector is an avalanche photodiode which is biased to provide a linear response to both the average reflected light and the small thermoreflectance signal. The linearity was checked by halving the incident light and observing the both the dc photocurrent and thermoreflectance signal were reduced by a factor of 2. The detected light is spectrally filtered to reject any scattered heating laser light. The heating laser pulse train is amplitude modulated by an electro-optic modulator driven with a 10-MHz sine wave. The heating laser is polarized parallel to the plane of incidence and it is focused onto the sample to a diameter of ≈ 20 μm. The 10-MHz modulation of the heating pulse train amplitude results in a thermomodulation of the reflected probe-pulse train, and the detector photocurrent modulation is measured by a lock-in amplifier tuned to 10 MHz.

The time-resolved thermoreflectance signal is obtained by fixing the probe wavelength and incrementally increasing the delay between the heating and probing pulses. The signal from the lock-in amplifier is divided by the detector dc signal to yield the fractional change in reflectivity, $\Delta R/R$. This procedure is repeated at different probe wavelengths with the heating wavelength fixed at 645 nm. The delay line scanning and data acquisition are performed by computer.

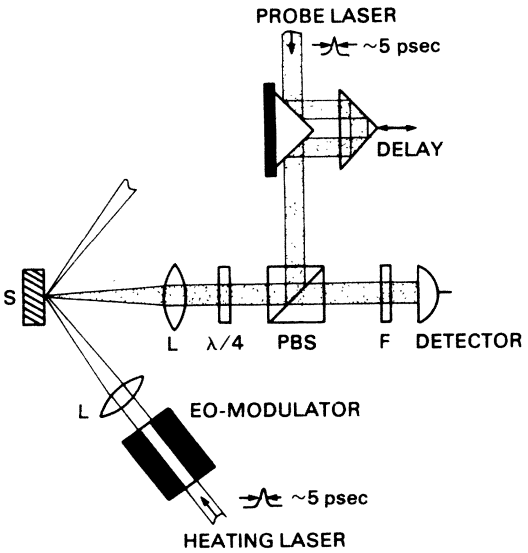

FIG. 2. Optical schematic of the transient thermoreflectance arrangement. L: lens; F: filter; PBS: polarization beam splitter; $\lambda/4$: quarter-wave plate.

TRANSIENT THERMOREFLECTANCE: COPPER

Transient thermoreflectance signals have been generated from a number of of sample structures, including evaporated, sputtered, and single-crystal Cu. Figure 3 shows the unusual transient thermoreflectance signals observed from a 400-nm-thick evaporated Cu film (supported by a CuZr mirror substrate). Thermoreflectance transients are shown for four different probe photon energies in the vicinity of the *d*-band absorption edge at 2.15 eV. The rapid transient which occurs at zero time delay essentially follows the cross correlation of the heating pulse with the probing pulse. The relatively long decay of $\Delta R/R$ in ≈ 200 psec corresponds to the diffusion of heat out of the optical skin depth region.[19] This suggests that the rapid component of the data is a result of direct electron heating and cooling on a time scale comparable to the heating pulse width. Although the *e*-ph collision time in Cu at room temperature is $\approx 2\times 10^{-14}$ sec (see Table I), an electron-energy relaxation time on the order of 10^{-12} sec would be expected. The large energy mismatch between a hot electron (≈ 1 eV) and a phonon (≈ 0.015 eV) requires several collisions for energy relaxation.[6]

The unique spectral response of the rapid transient can be explained by considering the heating-induced change in

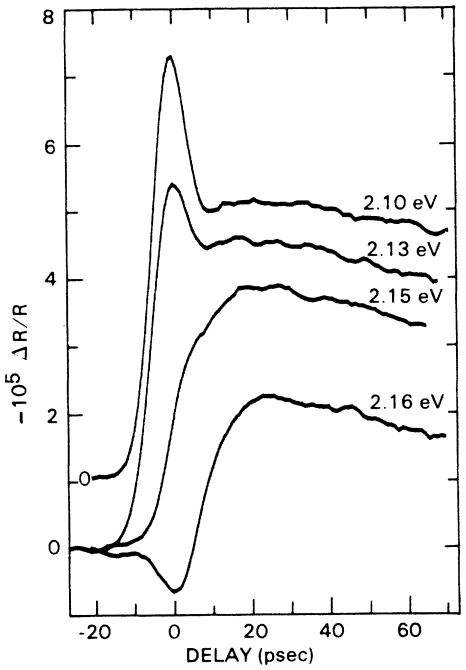

FIG. 3. Time-resolved $\Delta R/R$ transients for copper. Each transient is labeled by the probe photon energy, and the horizontal axis is the delay of the probe pulse relative to the heating pulse. The 2.10-eV transient is offset for clarity. The heating photon energy is 1.92 eV for all data.

TABLE I. Physical constants used for the calculations shown in Figs. 6 and 7.

Temperature	300 K	100 K
R: reflectivity[a]	0.92	0.92
K: thermal conductivity[b] (W/m K)	401	610
C_l: lattice heat capacity[b] (J/m^3 K)	3.43×10^6	2.26×10^6
A: electronic heat capacity[b] (J/m^3 K^2)	96.6	96.6
$\tau_{e\text{-ph}}$: electron-phonon collision time[c] (sec)	2.4×10^{-14}	7.4×10^{-14}
α: absorptivity[d] (m^{-1})	7.1×10^7	7.1×10^7
G: electron-phonon coupling [Eq. (4)] (W/m^3 K)	2.6×10^{17}	8.6×10^{16}
m: electron mass[b] (kg)	9.1×10^{-31}	9.1×10^{-31}
N: conduction-electron density[e] (m^{-3})	8.4×10^{28}	8.4×10^{28}
v: longitudinal sound velocity[b] (m/sec)	5010	5010
T_d: Debye temperature[b] (K)	343	343
D: Debye integral[f] [Eq. (5)]	0.62	0.20
I: laser intensity (W/cm^2)	50×10^6	50×10^6
τ: Gaussian pulse width ($1/e$ full width) (sec)	4×10^{-12}	4×10^{-12}
$\partial\rho/\partial T$: Fermi smearing [Eq. (1)] (K^{-1})	6.3×10^{-4}	6.6×10^{-5}

[a]Measured at a pump wavelength of 640 nm.
[b] *American Institute of Physics Handbook*, 3rd ed. (McGraw-Hill, New York, 1972).
[c]From the dc resistivity in footnote b.
[d]From $\alpha=4\pi k/\lambda$ [H. Hagemann, W. Gudat, and C. Kunz, J. Opt. Soc. Am. 65, 742 (1975)].
[e]C. Kittel, *Introduction to Solid State Physics*, 4th ed. (Wiley, New York, 1971), p. 248.
[f] *Handbook of Mathematical Functions*, edited by M. Abramowitz and I. A. Stegun (Dover, New York, 1970), p. 998.

the distribution of occupied electronic states near the Fermi level,[11,14]

$$\rho=1/(1+\exp\{[\tilde{h}\omega-(E_F-E_d)]/k_BT\}) . \quad (1)$$

These states directly affect the absorption of photons with energies ($\tilde{h}\omega$) which correspond to the transition of electrons from the top of the d band (energy E_d, see Fig. 1) to the Fermi level (E_F). When the conduction-electron temperature increases during the heating pulse, the Fermi distribution of *occupied* states decreases slightly for $\tilde{h}\omega<E_F-E_d$. That is, $d\rho/dT<0$ and more d-band electrons are promoted into the conduction band by the absorption of probe photons at these energies. This results in a *decrease* in the reflectivity for $\tilde{h}\omega<E_F-E_d$. At the same time, however, there is a heating-induced increase in the number of conduction electrons which occupy states above E_F; that is, $d\rho/dT>0$ for $\tilde{h}\omega>E_F-E_d$. We expect to see a heating-induced *increase* in the reflectivity since fewer empty conduction-band states are available for transitions from the d band. When the probe photon energy coincides with the d band to the Fermi-level transition energy (2.15 eV in Cu) there is no temperature modulation of the unoccupied states sampled; to first order $d\rho/dT=0$. The spectral behavior of $d\rho/dT$ is plotted in Fig. 4 for two different temperatures. We see that as the ambient temperature (T) of the conduction electrons is lowered, the spectral width of the Fermi distribution smearing ($d\rho/dT$) is reduced. In any case, there is no Fermi smearing for a probing photon energy of 2.15 eV, and changes in reflectivity will only result from lattice heating effects such as expansion and an increased electron-phonon collision frequency. This explains the absence of the rapid component in the 2.15-eV data of Fig. 3.

Confirmation of the nonequilibrium nature of the heating process can be made by comparing the spectral response of $\Delta R/R$ at different times. Figure 5 is a plot of (a) the peak height of the rapid Fermi smearing component at zero time delay; and (b) an average of the signal level between 39 and 42 psec, versus photon energy. The

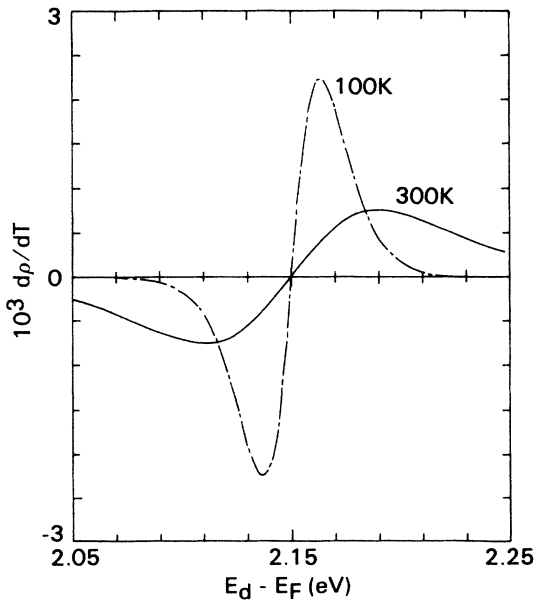

FIG. 4. Temperature derivative of the Fermi distribution ρ [Eq. (1)] versus the energy difference between the top of the d band and Fermi level in copper. The derivative is evaluated at 100 and 300 K, demonstrating the spectral broadening as temperature increases.

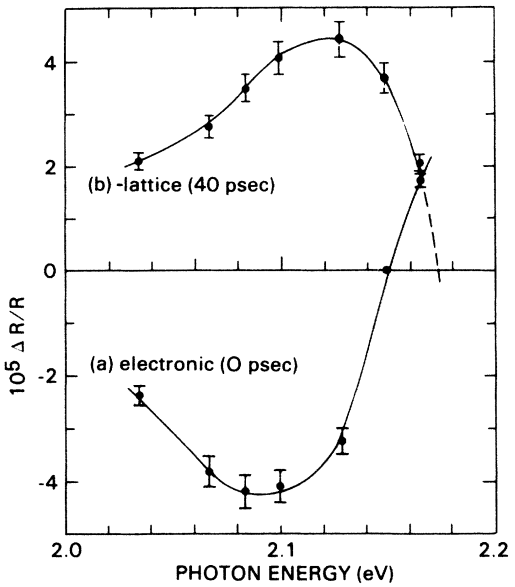

FIG. 5. Transient thermoreflectance spectra of copper: (a) peak height of the rapid contribution to the data in Fig. 3 (see text); (b) $-\Delta R/R$ at $\approx$40-psec time delay. Dashed line indicates expected behavior for larger photon energies.

rapid and slow components of the data in Fig. 3 are separated by scaling and subtracting the 2.15-eV data from all other delay scans at different photon energies. The result is a peak whose shape is nearly identical to the cross correlation of the probing pulse with the heating pulse, and the height of this peak provides the data for Fig. 5(a). The data in Fig. 5(b) (sign reversed for clarity) is representative of the lattice contribution to $\Delta R/R$, which includes not only expansion-induced changes in band structure and increased e-ph interactions, but also includes Fermi smearing of electronic states in equilibrium with the lattice temperature. Both spectra in Fig. 5 demonstrate the dominance of the Fermi smearing contribution (shown in Fig. 4) to the reflectivity change in this energy range. The fact, that the spectrum at zero time delay is down shifted in energy relative to the spectrum at $\approx$40 psec, indicates the presence of a nonequilibrium situation. The ratio of the Fermi-smearing contribution to the other $\Delta R/R$ contributions is larger during the heating pulse than it is 40 psec later. This implies that the electron temperature during the heating pulse exceeds the lattice temperature. As the lattice temperature increases following the heating pulse, the lattice contributions to the reflectivity change will offset the zero crossing point of the characteristic Fermi smearing line shape.

The ability to resolve the initial electron heating contribution to $\Delta R/R$ results from the use of probe photon energies which produce transitions from the d band to the Fermi level in Cu. Since the band structure shown in Fig. 1 is representative of the noble metals in general, we would expect to observe Fermi smearing transients from Au and Ag as well. Using probe photon energies near 2.15 eV, qualitatively similar transients have been observed from Au films where $E_F - E_d = 2.4$ eV. As a result of the large energy gap in Ag ($\approx$4 eV), no Fermi smearing transients are observed using $\approx$2.1-eV photons.

NONEQUILIBRIUM ENERGY BALANCE MODEL

The transient thermoreflectance measurements show that a short optical pulse is first absorbed by the electrons which thermalize rapidly and then cool by transfering energy to the lattice via electron-phonon scattering. If the heating pulse is long compared to the e-ph energy transfer time, the electrons and lattice will remain in thermal equilibrium and the temperature of the system will be described by the heat-conduction equation,[19]

$$C_i(dT/dt) = K\nabla^2 T(r,t) + P_a(r,t) \ . \tag{2}$$

In Eq. (2), C_i is the lattice heat capacity, K is the thermal conductivity, and $P_a(r,t)$ is the absorbed laser power density.

When a nonequilibrium temperature difference is generated by heating pulses shorter than the e-ph energy transfer time, the heating and cooling process must be modeled by a two-temperature system of coupled differential equations. For the case of one-dimensional heat flow into the sample (z direction) the macroscopic energy balance equations take the form,[1,2]

$$AT_e(dT_e/dt) = K(d^2T_e/dz^2) - G(T_e - T_i) + P_a(r,t) \ , \tag{3}$$

and

$$C_i(dT_i/dt) = G(T_e - T_i) \ , \tag{4}$$

where $T_e(r,t)$ is the electron temperature profile, $T_i(r,t)$ is the lattice temperature profile, $P_a(r,t)$ is the absorbed power density equal to $(1-R)\alpha I \exp^{-\alpha z} f(t)$, A is the electronic constant of heat capacity, K is the thermal conductivity, G is the electron-phonon coupling, C_i is the lattice heat capacity, α is the absorptivity, R is the reflectivity, I is the laser intensity, and $f(t)$ is the laser temporal profile. A one-dimensional heat-flow model is applicable to our thermoreflectance experiment since the laser focal diameters are sufficiently large that heat diffusion out of the optical skin depth ($\approx$20 nm) dominates over radial diffusion out of the illuminated area for time delays of several hundred picoseconds.

The electron and lattice temperatures in Eqs. (3) and (4) are coupled by the factor G (power density per unit temperature). G represents the electron-phonon coupling which can be calculated from theory based on the approximation of a free-electron metal with a Debye phonon spectrum.[1] If the lattice temperature is always less than the Debye temperature and the nonequilibrium electron-lattice temperature difference is small ($T_i < T_d$, $T_e - T_i \ll T_i$), then G may be determined from the equation,[1,2]

$$G = (\pi^2 m N v^2/6\tau T_i)(T_e/T_i)^4 \times \int_0^{T_e/T_d} [x^4/(e^x - 1)]dx \ , \tag{5}$$

where m is the electron mass, N is the conduction-electron density, v is the velocity of sound in the metal, τ is the e-ph collision time at T_i (from conductivity), and T_d is the Debye temperature. The relevant parameter for

determining if the coupled equation approach to the heat-flow problem is necessary is the ratio C_i/G [where G is calculated from Eq. (5)]. This ratio has units of time and if the heating pulse width is comparable to or less than C_i/G, then the coupled equation approach is necessary.

The solution to Eqs. (3) and (4) can be found by writing difference formulas and numerically solving for the electron and lattice temperature profiles.[6] Since the temperature differential generated in our experiment is small, we need not concern ourselves with changes in material parameters or nonlinear corrections to the temperature profiles and the resulting reflectivity change. The surface temperature profiles shown in Fig. 6 are calculated from Eqs. (3) and (4) using the Cu physical constants from Table I and the pulse parameters of the heating laser. For the heating pulse, we have assumed a Gaussian temporal profile with a pulse width of 4 psec ($1/e$ full width), and this is also plotted in Fig. 6.

Qualitatively, we find that the features of the actual measurements are reproduced by the calculation. We see that the peak lattice temperature in Fig. 6 is on the order of 1 K and that the peak electron-lattice temperature difference is only ≈ 2.2 K. This agrees with a relative comparison of our transient $\Delta R/R$ amplitudes to the equilibrium amplitudes measured by Rosei and Lynch.[14] They estimate a temperature modulation of ≈ 12 K is applied to their Cu sample, and they measure a $\Delta R/R \simeq 10^{-3}$. By comparison, our measured amplitude of $\Delta R/R \simeq 5\times 10^{-5}$ (at 20 psec, from Fig. 3) would scale to a temperature rise of $\Delta T \simeq 1$ K. This temperature rise would also be expected on the basis of the lattice specific heat, the illuminated volume ($V \simeq 4.4\times 10^{-18}$ m^3), and the absorbed laser pulse energy of $E_a = (1-R)\times 0.5$ nJ. That is, $\Delta T \simeq E_a/(VC_i) = 3$ K. We note that the results in Fig. 6 do not include the temporal broadening due to the finite width of the probing laser pulse which effectively convolutes these profiles in the transient reflectivity measurement.

These calculations show that nonequilibrium heating should be expected in our experiment, and that the real temperature excursions generated in the sample are on the same order as those calculated. Furthermore, since our experiment represents a very small perturbation to the material system, the above model for this situation is realistic. An unusual feature of the calculation shown in Fig. 6 is the undercooling of the electrons relative to the lattice at the surface of the metal. This result can be explained by the diffusion of hot electrons out of the surface region before equilibration. We do not believe this result is an artifact of the calculations procedure. Calculations for regions >50 nm below the surface do not display this undercooling effect.

Since the e-ph coupling parameter G is temperature sensitive, one might expect an observable change in the electron relaxation time as the sample is cooled. In fact, at 100 K the coupling factor [determined from Eq. (5)] is more than three times smaller than at 300 K. Thus it might be expected that at 100 K the rapid transient in Fig. 3 would exhibit a slower decay time, rather than follow the cross correlation of the heating and probing pulse. To test this conjecture, calculations were performed using the physical constants from Table I for a 100-K substrate temperature. The results are shown in Fig. 7, where we have evaluated the surface electron temperature for starting substrate temperatures of 300 and 100 K. In addition, the temperature profiles have been multiplied by the temperature derivative of the Fermi distribution evaluated at the starting lattice temperature and a probe photon energy of 2.09 eV (see Fig. 4). These calculations should be indicative of the Fermi smearing contribution to the reflectivity change at the two substrate temperatures.

For comparison, experimental results from TTRS measurements[10] on single-crystal Cu(110) at both 100 and 300 K are shown in Fig. 8. Again, we find that the experimental features are qualitatively reproduced by the calculations. In Fig. 7 the peak Fermi smearing signal at 100

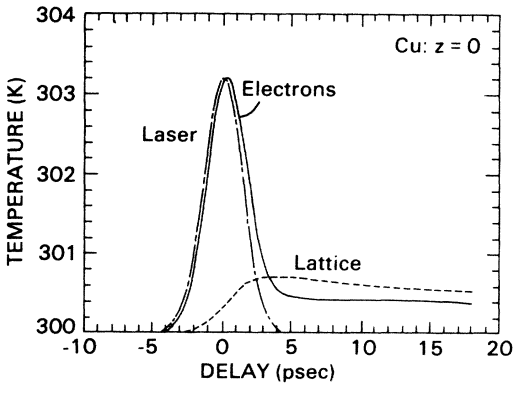

FIG. 6. Numerical solution of Eqs. (3) and (4) using a Gaussian laser pulse shape. The surface ($z=0$) electron temperature follows the solid line and the lattice temperature follows the dashed line.

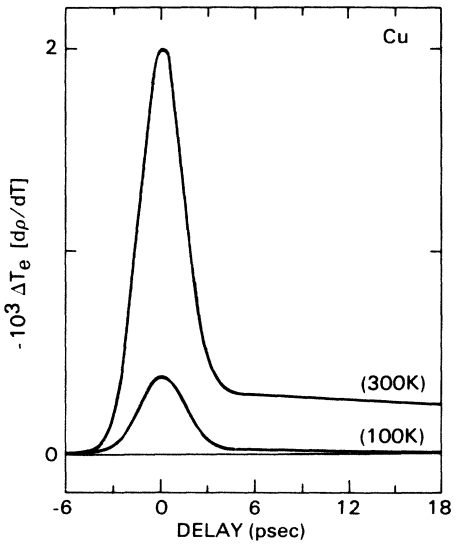

FIG. 7. Calculated surface electron heating multiplied by the Fermi smearing factor (evaluated at 2.09 eV; see Fig. 4), at substrate temperatures of 300 and 100 K. At 300 K the peak electron heating is 3.0 K above the lattice, and at 100 K the peak electron heating is 5.6 K above the lattice.

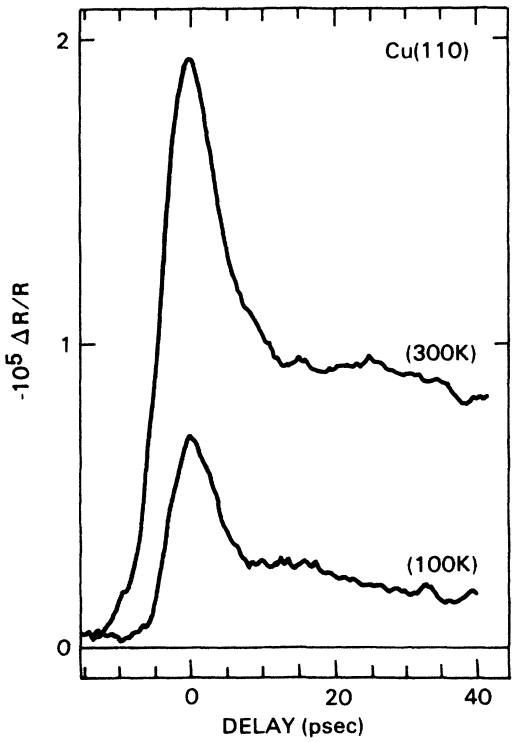

FIG. 8. Transient thermoreflectance signals from single-crystal Cu(110) at substrate temperatures of 300 and 100 K. The probe photon energy is 2.09 eV, permitting direct comparison with the calculations in Fig. 7.

K is approximately one-fourth that at 300 K. This trend is verified by the experimental results in Fig. 8, where the reduced signal at 100 K is offset by lattice contributions to $\Delta R/R$ which have not been included in the calculation (Fig. 7). As before, we have not included the convolving effect of the probe pulse on the calculated electron temperature profiles. Most importantly, we see that neither the experimental results nor the calculation show any significant broadening of the rapid transient as the substrate temperature is lowered and the e-ph coupling is reduced. This can be explained by the fact that the peak electron temperature excursion at 100 K is still small ($\sim$6 K), and although G is reduced, the e-ph coupling is still large enough to permit equilibration on the time scale of a few picoseconds.

As a final comment, we note that at 100 K we are nearing the anomalous skin depth regime for Cu.[20] That is, the e-ph mean free path is comparable to the optical skin depth and hot electrons can diffuse out of the heated region without equilibrating with the lattice. This diffusion-limited transport regime creates the possibility of using shorter laser pulses to investigate carrier transport in the presence of defects and impurities.

CONCLUSIONS

We have demonstrated a new method for obtaining the thermoreflectance spectra of metals. The picosecond time resolution of the current experiments permits the separation of electronic and lattice contributions to the reflectivity change. As a result, we have generated and observed the heating of metal electrons to a temperature above the lattice. We have shown that the small perturbation generated by the low-energy laser pulses can be modeled by separating the metal into electron and phonon subsystems and solving for the heat flow by a coupled-equation approach.

The confirmation of nonequilibrium heating in metals provides the basis for studying the relaxation kinetics of electrons with the lattice. Extension of the technique into the femtosecond time domain will provide the capability to directly measure hot electron relaxation times as a function of probe photon energy and temperature. Since the heating is produced optically, thick films and single crystals can also be studied.

More exciting is the opportunity to investigate the relaxation dynamics of the electron system near critical points in electronic phase transitions. For instance, experiments are in progress to monitor the spin dynamics of ferromagnetic materials near the Curie temperature. Similar experiments are conceivable for studying the relaxation dynamics of ferroelectric systems and superconducting systems. The key feature here is the generation of an electronic phase transition, while keeping the lattice below the transition temperature. From these considerations, we believe that the generation of transient nonequilibrium temperatures in metals will provide a test of the current theoretical understanding of carrier relaxation from a microscopic point of view. In addition, such experiments can yield new information about relaxation dynamics near critical points.

ACKNOWLEDGMENTS

I wish to thank B. Clemens, W. Capehart, and J. Fujimoto for helpful discussions during the course of this work. Comments on the manuscript from J. Buchholz, C. Paddock, and D. Lambert are also appreciated.

[1]M. I. Kaganov, I. M. Lifshitz, and L. V. Tanatarov, J. Exptl. Theor. Phys. (U.S.S.R.) 31, 232 (1956) [Sov. Phys.—JETP 4, 173 (1957)].

[2]S. I. Anisimov, B. L. Kapeliovich, and T. L. Perel'man, Zh. Eksp. Teor. Fiz. 66, 776 (1974) [Sov. Phys.—JETP 39, 375 (1974)].

[3]R. Yen, J. M. Liu, and N. Bloembergen, Opt. Commun. 35, 277 (1980).

[4]For a variety of examples, see *Picosecond Phenomena III*, Vol. 23 of *Springer Series in Chemical Physics*, edited by K. B. Eisenthal, R. M. Hochstrasser, W. Kaiser, and A. Laubereau (Springer, Berlin, 1982).

[5]M. B. Agranat, A. A. Benditskii, G. M. Gandel'man, P. S. Kondratenko, B. I. Makshantsev, G. I. Rukman, and B. M. Stepanov, Zh. Eksp. Teor. Fiz. **79**, 55 (1980) [Sov. Phys.—JETP **52**, 27 (1980)].

[6]R. Yen, Ph.D. thesis, Harvard University, 1981 (unpublished).

[7]J. G. Fujimoto, J. M. Liu, E. P. Ippen, and N. Bloembergen, Phys. Rev. Lett. **53**, 1837 (1984).

[8]S. I. Anisimov, V. A. Benderskii, and G. Farkas, Usp. Fiz. Nauk **122**, 185 (1977) [Sov. Phys.—Usp. **20**, 467 (1977)].

[9]G. L. Eesley, Phys. Rev. Lett. **51**, 2140 (1983).

[10]G. L. Eesley, in *Ultrafast Phenomena IV,* Vol. 38 of *Springer Series in Chemical Physics,* edited by D. H. Auston and K. B. Eisenthal (Springer, Berlin, 1984), p. 143.

[11]M. Cardona, *Modulation Spectroscopy* (Academic, New York, 1969), Chap. 5.

[12]W. J. Scouler, Phys. Rev. Lett. **18**, 445 (1967).

[13]E. Colavita, A. Franciosi, C. Mariani, and R. Rosei, Phys. Rev. B **27**, 4684 (1983).

[14]R. Rosei and D. W. Lynch, Phys. Rev. B **5**, 3883 (1972).

[15]R. Rosei, C. H. Culp, and J. H. Weaver, Phys. Rev. B **10**, 484 (1974).

[16]R. Rosei, F. Antonangeli, and U. M. Grassano, Surf. Sci. **37**, 689 (1973).

[17]C. G. Bethea, C. Y. Chen, A. Y. Cho, P. A. Barbinski, and B. F. Levine, Appl. Phys. Lett. **42**, 682 (1983).

[18]J. Kluge, D. Wiechert, and D. Von Der Linde, Opt. Commun. **51**, 271 (1984).

[19]J. H. Bechtel, J. Appl. Phys. **46**, 1585 (1975).

[20]F. Wooten, *Optical Properties of Solids* (Academic, New York, 1972), p. 93.

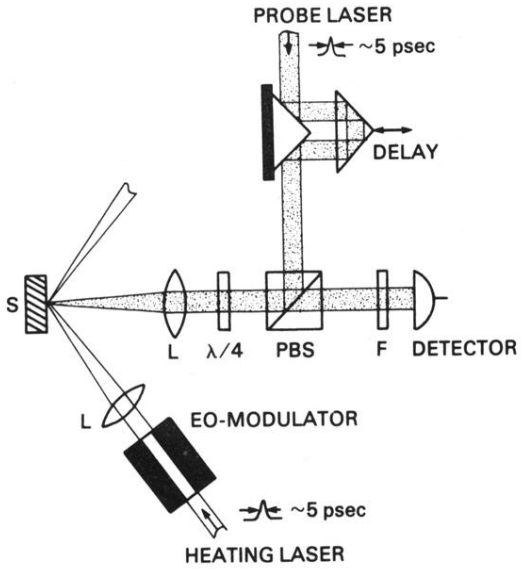

FIG. 2. Optical schematic of the transient thermoreflectance arrangement. L: lens; F: filter; PBS: polarization beam splitter; $\lambda/4$: quarter-wave plate.